Neurobiology of Aging 35 (2014) 2562–2573

Contents lists available at ScienceDirect

Neurobiology of Aging

journal homepage: www.elsevier.com/locate/neuaging

Choriocapillaris breakdown precedes retinal degeneration in age-related macular degeneration☆

Antje Biesemeier[a,*], Tatjana Taubitz[a], Sylvie Julien[a], Efdal Yoeruek[b], Ulrich Schraermeyer[a]

[a] Section for Experimental Vitreoretinal Surgery, Center for Ophthalmology, University of Tuebingen, Tuebingen, Germany
[b] Cornea Bank, Center for Ophthalmology, University of Tuebingen, Tuebingen, Germany

ARTICLE INFO

Article history:
Received 16 September 2013
Received in revised form 23 April 2014
Accepted 2 May 2014
Available online 10 May 2014

Keywords:
Age related macular degeneration
Choriocapillaris
Retinal pigment epithelium
Transition between healthy and atrophied areas
Whole-section panorama images

ABSTRACT

This work presents a combined light and electron microscopical approach to investigate the initial breakdown of the retinal pigment epithelium (RPE) and choriocapillaris (CC) in age-related macular degeneration (AMD). Perimacular sections of 12 dry and wet AMD eyes (82 ± 15 years) and 7 age-matched controls (75 ± 10 years) without retinal pathology were investigated. Disease progression was classified into 5 stages of retinal degeneration to investigate the concurrent CC breakdown. Special emphasis was laid on transitions where intact CC–RPE–retina complexes went over into highly atrophied areas. AMD sections showed elevated loss of photoreceptors, RPE and CC ($p < 0.01$), and thickened Bruch's membrane with increased basal laminar and linear deposits compared with controls. Up to 27% of the CC was lost in controls although RPE and retina were still intact. This primary loss of CC further increased with AMD (up to 100%). The data implicate that CC breakdown already occurs during normal aging and precedes degeneration of the RPE and retina with AMD, defining AMD as a vascular disease. Particular attention should be given to the investigation of early AMD stages and transitional stages to the late stage that reveal a possible sequence of degenerative steps with aging and AMD.

1. Introduction

Age-related macular degeneration (AMD) is the major cause of vision loss in the elderly individuals of the western world (Kocur and Resnikoff, 2002; Prokofyeva and Zrenner, 2011). It is a multifactorial late-onset disease (Herrmann et al., 2013), the main factors being smoking, obesity, and genetic predisposition (Liu et al., 2012), but primarily aging. AMD is characterized by changes in the retinal pigment epithelium (RPE), Bruch's membrane (BM), and choriocapillaris (CC), which together facilitate retinal degeneration predominantly in the macular region of the eye.

The RPE and CC share a mutualistic relationship, if one is compromised, the other will follow and thus both may degenerate within a short time of each other (Bhutto and Lutty, 2012). Many research and review articles have addressed the factors for onset and progression of AMD in the last 10 years, however, the actual order of degeneration in the choroid–RPE–retina interface is still not fully understood (Bhutto and Lutty, 2012; Lutty et al., 1999).

Actually, also in the brain, loss of microvascular density and basement membrane thickening with aging precede cerebrovascular dysfunction and successive age-related neurodegeneration, for example, in vascular dementia and Alzheimer's disease (Brown and Thore, 2010). Smoking, obesity, and hypertension contribute to both Alzheimer's disease (Sierra, 2012) and AMD, and both diseases are associated with amyloid and heavy metal deposition. These examples already reflect the obvious, but until now rarely studied communalities within these and other age-related neurodegenerative disorders. The present work aimed to investigate different stages of AMD in human donor eye tissue by light and electron microscopy to find out whether CC breakdown precedes RPE degeneration with age and AMD. In addition, high-resolution overview images of AMD histology are presented, which show sites of the degenerating retina which are directly facing other areas with surviving photoreceptors (Supplementary Figs. 1–3).

2. Methods

2.1. Donor eyes

Perimacular regions (about 7 mm from the foveal center) of 12 AMD donor eyes (8 wet AMD; 4 dry AMD) and 23 controls without known ophthalmic pathology were excised and fixed for electron

* Corresponding author at: Section for Experimental Vitreoretinal Surgery, Center for Ophthalmology, University of Tuebingen, Schleichstr.12/1, 72076 Tuebingen, Germany. Tel.: +49 7071 2984774; fax: +49 7071 4554.
E-mail address: antje.biesemeier@med.uni-tuebingen.de (A. Biesemeier).

0197-4580/$ – see front matter © 2014 The Authors. Published by Elsevier Inc. All rights reserved.
http://dx.doi.org/10.1016/j.neurobiolaging.2014.05.003

Table 1
Donor demographics and overview of measured stages I–V

Donor number	Age (y)	Sex	AMD type	Postmortem time (h)	Cause of death	Stages investigated
A1	71	M	Wet	7	Unknown	II, II–IV, IV
A2	72	F	Dry	48	Cerebral vascular infarction	II, II–IV, IV
A3	74	F	Wet	10	Liver cancer	II, II–IV, IV
A4	75	F	Wet	9	Septic shock secondary to urinary tract infection	II, II–III, III
A5	76	M	Wet	9.5	Respiratory failure, COPD	III, III–V, V II, II–V, V
A6	80	M	Wet	6.5	Pneumonia	V, V, V
A7	83	F	Wet	13	Unknown	II, II–IV, IV
A8	84	M	Dry	7.5	COPD, seizure	II, II, II
A9	90	F	Dry	11	Colicystitis, presented to ER	II, II–IV, IV
A10	91	F	Wet	23.5	CAD-MI	II, II–IV, IV–V, V
A11	93	F	Dry	7	Congestive heart failure	II, II–IV, IV
A12	100	F	Wet	7	Leukemia	I, I–II, II–V, V

Key: AMD, age-related macular degeneration; CAD-MI, coronary artery disease-myocardial infarcation; COPD, chronic obstructive pulmonary disease; F, female; M, male.

microscopy (EM). If possible, the samples were excised right at the border between atrophied and healthier regions (only in AMD eyes) to facilitate investigation of the transition areas.

2.1.1. AMD eyes

Glutaraldehyde-fixed tissue samples of the perimacular central region of 12 AMD donor eyes (age 71–100 years; mean 82 ± 15 years; Table 1) were obtained from the Cole Eye Institute of the Cleveland Clinic Foundation (USA). The death to fixation time was 13 ± 12 hours. The eyes were investigated by experienced ophthalmologists who stated the AMD type of both eyes including the different types of lesions found in each eye. The pathology reports also stated the cause of death and further diseases. Written informed consent of the donors for use in medical research and additional approval of the Institutional Review Board of the University of Tuebingen were obtained. The experiments were performed in adherence to the tenets of the Declaration of Helsinki.

2.1.2. Control eyes

Healthy donor eyes without known ophthalmic diseases were sectioned and investigated histologically. All eyes showing increased age-related lesions like RPE detachment or outer segment loss, or even geographic atrophy (GA) or choroidal neovascularization (CNV) and thus, resembling clinically unrecognized AMD or another pathology were excluded from the cohort of control eyes. Finally, 9 age-matched eyes aged 57–85 years (mean age 75 ± 10 years; death to fixation time 19 ± 10 hours; not significant [NS] to AMD) were integrated in this study and served as healthy controls (Table 2).

The eyes were obtained from the Institute of Anatomy and the Eye Hospital Tuebingen with informed consent of the donors and approval of the Institutional Review Board of the University of Tuebingen. They were opened with a circular slit at the limbus and fixed overnight at 4 °C in 4% glutaraldehyde in 0.1 M cacodylate buffer (pH 7.4). Then the iris and vitreous were removed and the perimacular region was excised according to the AMD samples and further prepared for EM as follows.

2.2. Embedding

Small pieces (1.5 mm^3) of already fixed perimacular tissue samples were washed 3 times in 0.1 M cacodylate buffer, postfixed in 1% osmium tetroxide, stained with uranyl acetate and dehydrated in a graded series of ethanol and propylenoxide and embedded in Epon. All EM reagents were purchased from FLUKA (Sigma-Aldrich, St. Louis, MO, USA) and PLANO (Wetzlar, Germany).

2.3. Correlative light and electron microscopy

For each eye, one representative 2–3 mm long semithin perimacular section of the retina–choroid complex was stained with toluidin blue and completely photographed with 600× magnification by light microscopy. The images were rearranged with the photomerge function of Adobe Photoshop CS3 or the Microsoft ICE tool yielding a panorama overview containing up to 200 single images (examples in Figs. 1–6 and the Supplementary Figs. 1–3, with about 50 single images each). By zooming into this panorama, different topics were addressed individually and in context with the surrounding tissue. For example, the presence or absence of photoreceptors, RPE, basal deposits, and CC were quantified in whole semithin sections (about 2–3 mm length of BM), within central areas of the single stages and, if apparent, directly at the transitions (investigated over a length of 200 μm of BM; frames in Fig. 1A).

Three subsequent ultrathin sections were investigated by EM yielding subcellular information of the same area, for example,

Table 2
Control donor demographics. All donors showed foremost stage II

Donor number	Age (y)	Sex	AMD type	Postmortem time (h)	Cause of death	Stages investigated
C1	57	M	No AMD	16	Hemorrhagic shock	I, I, I
C2	67	F	No AMD	21	Respiratory failure	I, I–II, II
C3	68	F	No AMD	6	Massive hemorrhage	II, II, II
C4	75	M	No AMD	38	Cerebral edema	II, II, II
C5	78	M	No AMD	21	Circulatory failure	I, I–II, II
C6	80	M	No AMD	22	Aspiration and/or laryngeal cancer	II, II, II
C7	80	M	No AMD	26	Circulatory failure	II, II, II
C8	81	M	No AMD	8	Cardiac failure	II, II, II
C9	85	F	No AMD	Unknown	Unknown	II, II, II

Key: AMD, age-related macular degeneration; F, female; M, male.

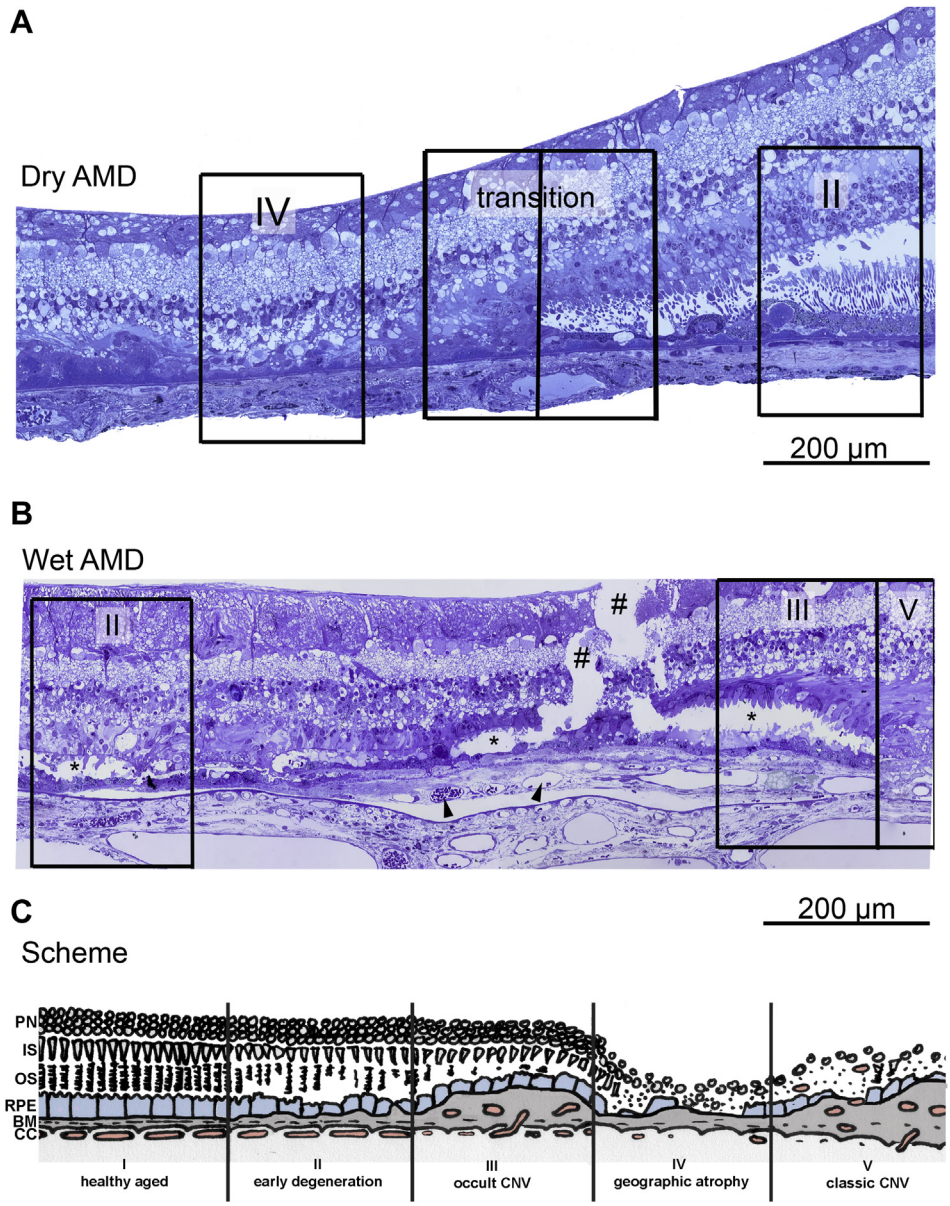

Fig. 1. The 5 stages of degeneration in AMD. (A) Light microscopical panorama image of a section from a dry AMD donor: shown is a transition between a highly atrophied region on the left (photoreceptors, RPE, and CC lumina are completely absent) and a histologically complete area on the right (complete photoreceptors, confluent RPE, open capillaries, basal deposits begin to detach the RPE from the BM). According to the scheme in (C) they were defined as stages IV and II, respectively. (B) Light microscopical panorama image of a section from a wet AMD donor: on the left, the RPE is still in contact with the Bruch's membrane and is separated from the photoreceptors by a subretinal space (*, stage II). This area goes over into an area with occult CNV as the RPE layer is separated from the Bruch's membrane by a CNV sheet with newly formed blood vessels (arrowheads). In the center region of stage III, some photoreceptor inner segments are still recognizable. On the right, stage III goes over into stage V, where the RPE and photoreceptor layer have completely disappeared leaving behind the CNV vessels and a retinal scar. The choroid shows highly enlarged deeper blood vessels and only a few melanocytes. # Breaks are sectioning artefacts. (C) Diagram showing the 5 histologic stages categorized for this work. They are based on RPE and photoreceptor ultrastructure and used for follow-up investigation of CC loss. A relation to inner retinal layers was not intended and thus of the retinal layers only the photoreceptors are shown. Stage I: control histology showing complete photoreceptors, an even RPE monolayer and regular CC vessels; basal deposits if apparent are few in number or very thin. Stage II: age-related changes shown by lost outer segments, RPE detachment or hypertrophy, basal deposits, enlarged Bruch's membrane or loss or shrinkage of CC vessels. Stage III: occult CNV with newly-formed capillaries between CC and RPE. Stage IV: geographic atrophy with loss of photoreceptor inner and outer segments, RPE, and CC vessels. If basal deposits are present, this stage is also associated with remnant basal deposits (as shown in (A). Stage V: classic CNV with newly formed blood vessels growing into the retina through the, not always present, RPE layer (see digital version for color images). High-resolution whole section panorama images of the tissues illustrated in A and B are provided in the Supplementary Figs. 1 and 2, respectively. Abbreviations: AMD, age-related macular degeneration; BM, Bruch's membrane; CC choriocapillaris; CNV, choroidal neovascularization; IS, inner segments; OS, outer segments; PN, photoreceptor nuclei; RPE, retinal pigment epithelium.

integrity of the endothelium and number of fenestrations. If a panorama overview was also needed for the EM investigations, for example, for proper investigation of vessels and photoreceptors within the same image, it was made using the multiple image alignment function of the iTEM 5.0 (Olympus) software (Fig. 6B). Of each one representative semi and ultrathin section per donor, semiquantitative evaluations were performed as follows (2.4–2.7).

2.4. Grading of histologic stages

After a first examination of both AMD and control panorama overviews, 3 independent areas of 200 µm length were selected per section, and each graded in 1 of 5 stages of retinal and RPE degeneration by 2 independent researchers. The stages were defined as follows:

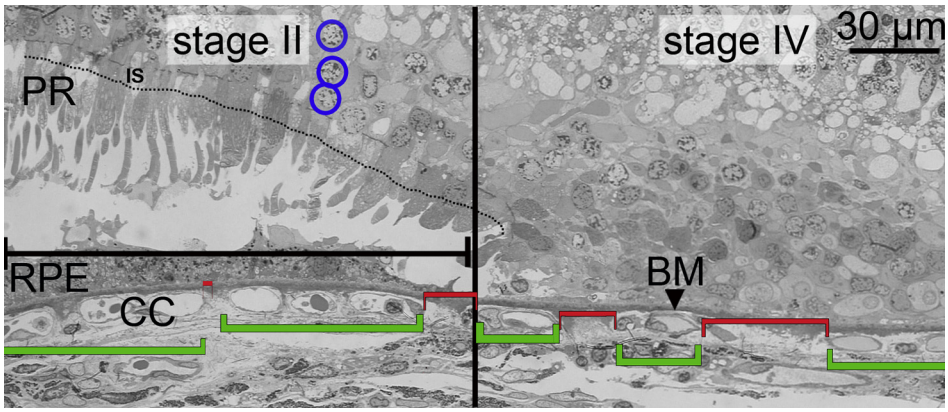

Fig. 2. Light microscopic image of how CC and RPE layer presence were measured: almost 100% of Bruch's membrane (arrowhead) is covered with RPE cells in the stage II area, whereas the RPE is missing completely in the stage IV area. The choriocapillaris was measured as follows: the green brackets (⌊⌋) include the vessel lumina plus the endothelium and typical pillars with a width of less than 10 µm. The red brackets (⌐¬) illustrate the areas of degenerated (no endothelium) or shrunken capillaries, which can be empty or contain extracellular matrix or alien cells. In stage II, about 90% of the CC is present, whereas in stage IV about 40% of the CC has disappeared. Photoreceptors (PR) were measured as follows: nuclei were counted in rows (filled circles), inner segments per µm BM, (dotted line) and outer segments per µm BM (as the inner segments, not shown) (see digital version for color and magnified images). The whole section panorama image of this donor tissue is presented in Supplementary Fig. 3). Abbreviations: BM, Bruch's membrane; CC choriocapillaris; RPE, retinal pigment epithelium.

Stage I: healthy (photoreceptors contain clearly distinguishable inner and outer segments, the RPE builds a continuous monolayer, no, or few deposits between the RPE and Bruch's membrane).

Stage II: normal age-related early retinal and RPE damage, that is, either changes in the structure of photoreceptors (shortened outer segments, first loss of photoreceptors foremost at transitions of AMD sections) or an irregular or hyperplastic but still confluent RPE monolayer or thickened BM.

All control sections used in this study were selected to fit in one of the first 2 stages I and II. Samples of control donors, which showed any AMD-related pathology like RPE or retinal degeneration were excluded from the examination.

Stage III: occult CNV (or type 1 neovascularization [Freund et al., 2010]), that is, blood vessel outgrowth through a thickened BM, with vessels close to the RPE but not infiltrating the subretinal space. Photoreceptors already impaired, but present.

Stage IV: GA, that is photoreceptor outer segments, inner segments, and the RPE are completely absent and degenerated leaving behind only single cells if any. The subretinal space is more or less abolished when the outer nuclear layer is touching Bruch's membrane.

Stage V: classic CNV (or type 2 neovascularization [Freund et al., 2010]), that is, the outgrowth of blood vessels through the not always present RPE layer into a highly damaged retina.

These 5 stages were put into a scheme, which is illustrated in Fig. 1c. This scheme is adapted from Sarks (1976) and shows the progression of the disease as a function of RPE and retinal destruction.

Seven sections of 7 different AMD donors were investigated more thoroughly, yielding changes in the RPE and choriocapillaris directly at transitions between different stages (Fig. 2). Transitions from stages II–IV were most common (5 donors), followed by stage II–V (2 donors). Transitions from I to II, IV to V and III to V occurred only once.

The following questions were addressed:

1) CC breakdown was investigated in relation to the RPE or retinal presence to answer the question whether the RPE or CC dies first with AMD progression.
2) The same stage of AMD progression was investigated and compared with samples of different donors, for example, differences in stage II of donors with dry or wet AMD help to explain the progression in the given direction.

2.5. Quantification of photoreceptors, RPE, BM, and CC

Fig. 2 shows how transition stages between healthier and more damaged areas, here stage II to stage IV, were analyzed. The spaces covered by photoreceptors, RPE, basal deposits, or CC were investigated and correlated to each other using the common unit "percent of BM length". This nomenclature gives no information about the morphology or quality of tissue, but it indicates whether a certain tissue layer is present or absent in this area. Using this approach, the "kinetics" of degeneration, for example, whether the RPE or CC fades away first were investigated histologically.

2.5.1. Measurement of photoreceptors

The area covered by outer and inner segments was measured per µm length of BM in semithin sections. Photoreceptor nuclei were counted in nuclei per row.

2.5.2. Bruch's membrane and basal depositions

The thickness of BM was measured in the semithin sections at 3 positions per section yielding the distance between the CC basal membrane and the RPE basal membrane. If BM was thickened, that area was investigated on a semiquantitative basis as performed in Curcio et al. (1998) and van der Schaft et al. (1992): that is, (0) no deposit, (1) patchy deposit <125 µm length, (2) thin continuous with >125 µm length and <2 µm height, (3) thick continuous with >2 µm height. The type of deposit (linear, laminar) was addressed at $20,000\times$ magnification in the EM. Basal linear deposits (lin) were defined as being between the RPE basal lamina and the inner collagenous layer of BM (Green and Enger, 1993). Basal laminar deposit was defined as being between the RPE basal lamina and the RPE cell membrane (Loffler and Lee, 1986).

2.5.3. Measurements in the CC

The areas of the lumina of the CC capillaries were measured ($\mu m^2/\mu m$ BM). Additionally, 2 markers for CC integrity, fenestration and length of CC layer present were addressed as follows.

The number of fenestrations per µm of CC endothelium was counted in 30 images with $50,000\times$ magnification. Only fenestrations facing the RPE side were counted, also if further fenestrations were visible on the choroid-faced side.

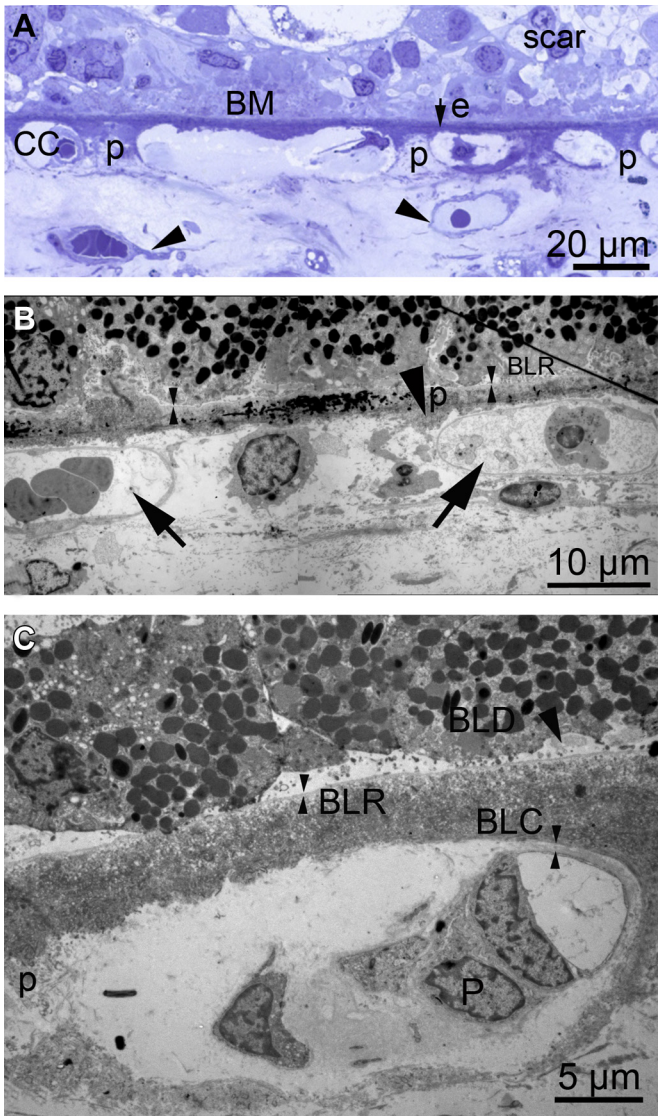

Fig. 3. Loss of choriocapillaris vessels. (A) Light microscopical image of geographic atrophy in AMD. Photoreceptors and the RPE are completely lost, leaving a scar. The CC is highly impaired, only one shrunken capillary (resembling that shown in (C) remains on the left side), whereas the CC is completely absent in the rest of the image showing foremost ghost vessels with loss of endothelia. The arrowheads point to deeper choroidal vessels with intact endothelia. Nevertheless, typical pillars (p) can be recognized showing where the vessels were originally situated. Using LM, the elastica of Bruch's membrane (BM) can be clearly recognized (e). (B) EM image of an AMD section where 1 capillary is entirely lost between 2 complete capillaries (black arrows). The space left is filled with macrophage-like cells. The arrowhead points to a pillar (p). By EM, BM can further be investigated: the elastic layer is calcified, basal laminae of RPE (BLR) and CC are not always discernible and fuse with the collagenous material. (C) EM image of another AMD eye, where a choriocapillaris lumen has shrunk to about 1/4 of its original size. Its basal membrane (BLC) surrounds only the small remaining capillary. The space between the remaining vessel and the original flanking pillar (p) is not yet filled with extracellular material. BM is slightly thickened, only the basal membrane of the RPE (BLR) is still completely discernible. Basal laminar deposits (BLD-arrowhead) are present. Abbreviations: AMD, age-related macular degeneration; CC choriocapillaris; EM, electron microscopy; LM, light microscopy; RPE, retinal pigment epithelium.

The whole length of the capillary layer including endothelial cell bodies and pillars was quantified (Fig. 2). CC was defined as being present when the capillaries were covered by a light microscopically visible endothelium and filling the whole space between 2 pillars of Bruch's membrane (green brackets in Fig. 2 ⌊⌋). If a capillary was shrunken, that is, a space appeared between pillar and endothelial wall, or a vessel was completely absent (no capillary on a length of more than 10 µm between neighboring capillaries) then this area was defined as lacking CC (red brackets in Fig. 2 ⌐¬). If unclear, this was controlled by EM. Examples of such absent or shrunken capillaries in higher magnification are illustrated in Fig. 3. In comparison to measuring only the area of CC vessel lumina, this approach yields additional information on the overall composition and integrity of the whole CC layer and thus more accurately describes CC density. It is also less vulnerable for postmortem artefacts like capillary collapse. Percent coverage of CC length can also more easily be compared with RPE length as it is used in the analyses for Figs. 7–9, where local degradation of either RPE and/or CC is investigated.

2.6. Statistical analysis

Statistics were performed using either Student *t* test for parametric analyses or the Wilcoxon–Mann–Whitney test for nonparametric data sets. The null hypothesis was that the AMD affected samples were histologically not different from the control samples. All *p*-values <0.05 were stated significantly different (error probability 5%). Linear regression analyses yielded the interdependency of RPE and CC survival in the different stages.

3. Results

3.1. Whole section analysis

Histologic changes in AMD compared with healthy control were addressed in whole perimacular sections of 12 AMD donor eyes and 9 control eyes.

All control sections did fit in one of the 2 first stages I and II. They showed a complete retina and RPE over section length (each about 100%), basal deposits were not present or few in number and area, leading to a mean thickness of BM of 3 ± 1 µm.

Compared with controls, AMD sections showed areas with loss of photoreceptors (nuclei, inner, and outer segments, all $p < 0.01$), RPE ($p = 0.009$), and CC ($p < 0.0001$). Bruch's membrane was thickened and basal deposits were more pronounced in AMD sections ($p = 0.006$ to controls).

In 7 of the 12 AMD sections such degenerative areas were directly facing other areas with intact retina–choroid complexes. These transitions are described in detail in Section 3.2.

3.1.1. Choriocapillaris

Loss of choriocapillaris density was identified as empty spaces beside shrunken capillaries or enlarged pillars (Fig. 3). With AMD, the areas covered by CC lumina were halved in value compared with controls ($p < 0.0001$, Fig. 4A and B). Also the number of fenestrations in the remaining vessel endothelia was greatly decreased ($p < 0.0001$, Fig. 4C and D). A detailed analysis of CC breakdown in relation to the RPE is presented in Section 3.2 (Figs. 8 and 9).

3.1.2. Bruch's membrane and basal deposits

Semithin sections revealed the thickness of Bruch's membrane and the abundance of basal deposits, whereas EM sections clarified whether basal laminar or linear deposits were accumulating (Fig. 5). In Table 3, the results per donor are presented. Healthy control sections showed foremost small amounts of deposit formation, which were predominantly composed of basal laminar material. The AMD samples showed higher amounts of deposit formation, which were often continuously spread over the whole section length. All contained laminar deposits.

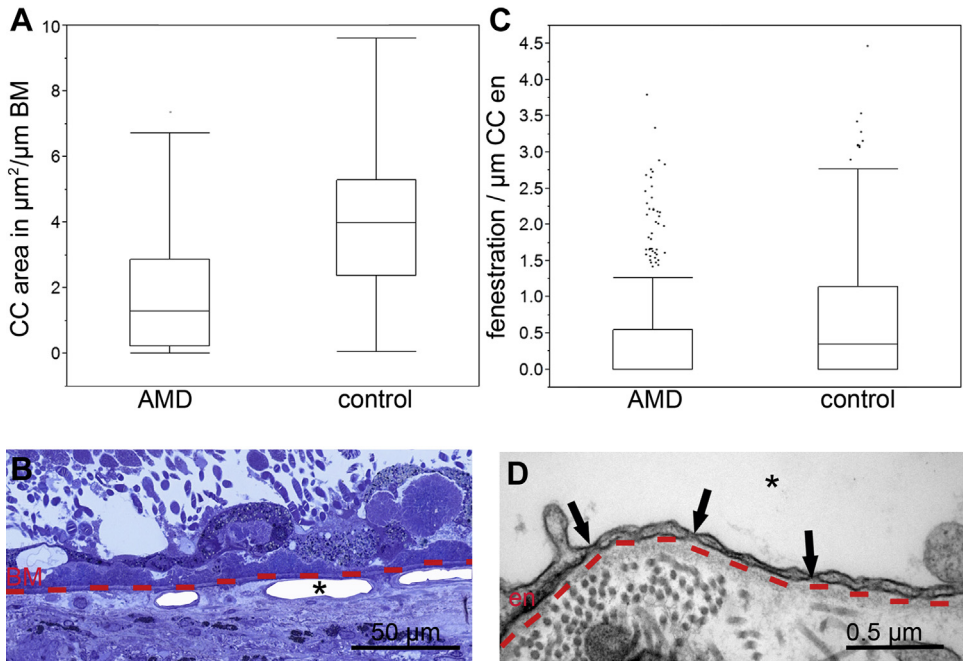

Fig. 4. Changes in the choriocapillaris. (A, B) Light microscopical analysis of CC area in $\mu m^2/\mu m$ BM (dashed line), $p < 0.0001$. CC lumina are shaded white and marked with an asterisk. (C, D) Electron microscopical analysis of CC fenestration (arrows) per µm length of the CC endothelium (dashed line, en). The asterisk marks the CC lumen, $p < 0.0001$. (see digital version for color images). Abbreviations: BM, Bruch's membrane; CC choriocapillaris.

3.1.3. Retinal pigment epithelium

The RPE was present in controls and early AMD but completely lost in areas of severe degeneration (97% ± 7% present in control; 63.7% ± 27% present in AMD sections; $p = 0.009$ to control).

In the earlier AMD stages, the RPE showed more morphologic changes rather than the absence of cells. The cells were often hypertrophic, microvilli clumped together or completely absent. Heavy deposition of basal waste was often associated with basal detachment of single, hypertrophic cells into the subretinal space. However, areas where the photoreceptors were already completely degenerated and the nuclei of the remnant retinal cells did reach to the underlying tissue were also free of the RPE in most cases. In these areas, the subretinal space had completely collapsed. On the other hand, when the subretinal space was still separating the degenerating photoreceptors from the underlying tissue, the RPE was also still present (Figs. 1 and 6, Supplementary Fig. 2).

3.1.4. Photoreceptor layer

The photoreceptors of AMD donors were highly degenerated as compared with those in controls (Table 4). When investigating photoreceptor loss, it was obvious that outer segments were the first to be lost with AMD. Already in stage II, first lesions could be observed, but mainly at the transitions going over into more damaged areas (stage II, 64% ± 42% of BM; stage IV, 0%). The inner segments were much more robust but absent with late stage AMD (stage II 76% ± 33% BM; stage IV 10% ± 22% BM). Photoreceptor nuclei were also lost with late stage AMD (6 ± 2 rows of nuclei in controls; IV 2.8 ± 3 rows of nuclei; V 0 rows;). Statistics showed significances between stages I or II as compared with stages IV and V, respectively (all $p < 0.001$).

In the late stage CNV, surviving photoreceptors, where just the outer segments were missing, were only observed at 3 small areas (80–500 µm; Fig. 1B, Fig. 6A and B, and Supplementary Fig. 2). Here, the RPE cells were also still present forming a continuous layer and were separated from the photoreceptors by a clearly recognizable subretinal space. However, up to 50-µm thick CNV sheets separated them from the remnant CC vessels. These comparatively healthy areas were surrounded by otherwise highly degenerated neovascularization scars. In the morphologically more intact areas, functional CNV vessels (defined as containing an intact endothelium, an open lumen and pericytes, and optionally with red blood cells; vessels 2–4 in Fig. 6A–C) were also observed more frequently than in scar tissue, where CNV vessels were often degenerating and showed leaky endothelia as judged by either loss of cell connections or death of whole endothelial cells (Fig. 6D and E, and Supplementary Fig. 2). CNV vessel morphology resembled mostly that of capillaries of the CC, but often they also displayed very large lumina and endothelial walls of different thickness. In addition, artery-like and venule-like vessels were observed. Typical pericytes such as that shown in Fig. 6C were seldom seen, but fibroblast-like cells were often found accompanying the endothelial membrane of CNV vessels (Fig. 6D and E).

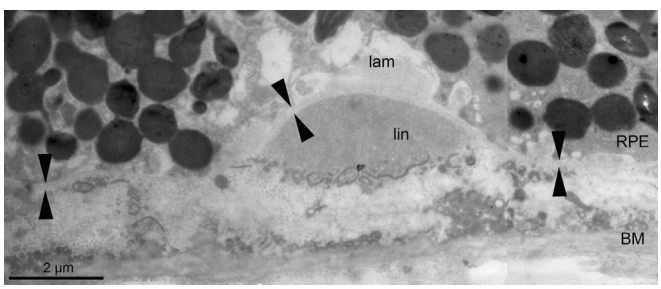

Fig. 5. EM micrograph of an AMD eye showing basal deposits: basal laminar deposits (lam) are located between the basal membrane of the RPE (arrows) and the RPE labyrinth. Basal linear deposits (lin) reside between the basal membrane of the RPE and the inner collagenous layer of Bruch's membrane (BM).

3.2. Analysis of transitional stages

3.2.1. Combined analysis of choriocapillaris and RPE in transition stages

Outside of transitions, areas where either the RPE or CC was missing whereas the other survived were equally abundant, thus a primary destruction of either tissue was hard to identify. Thus, the

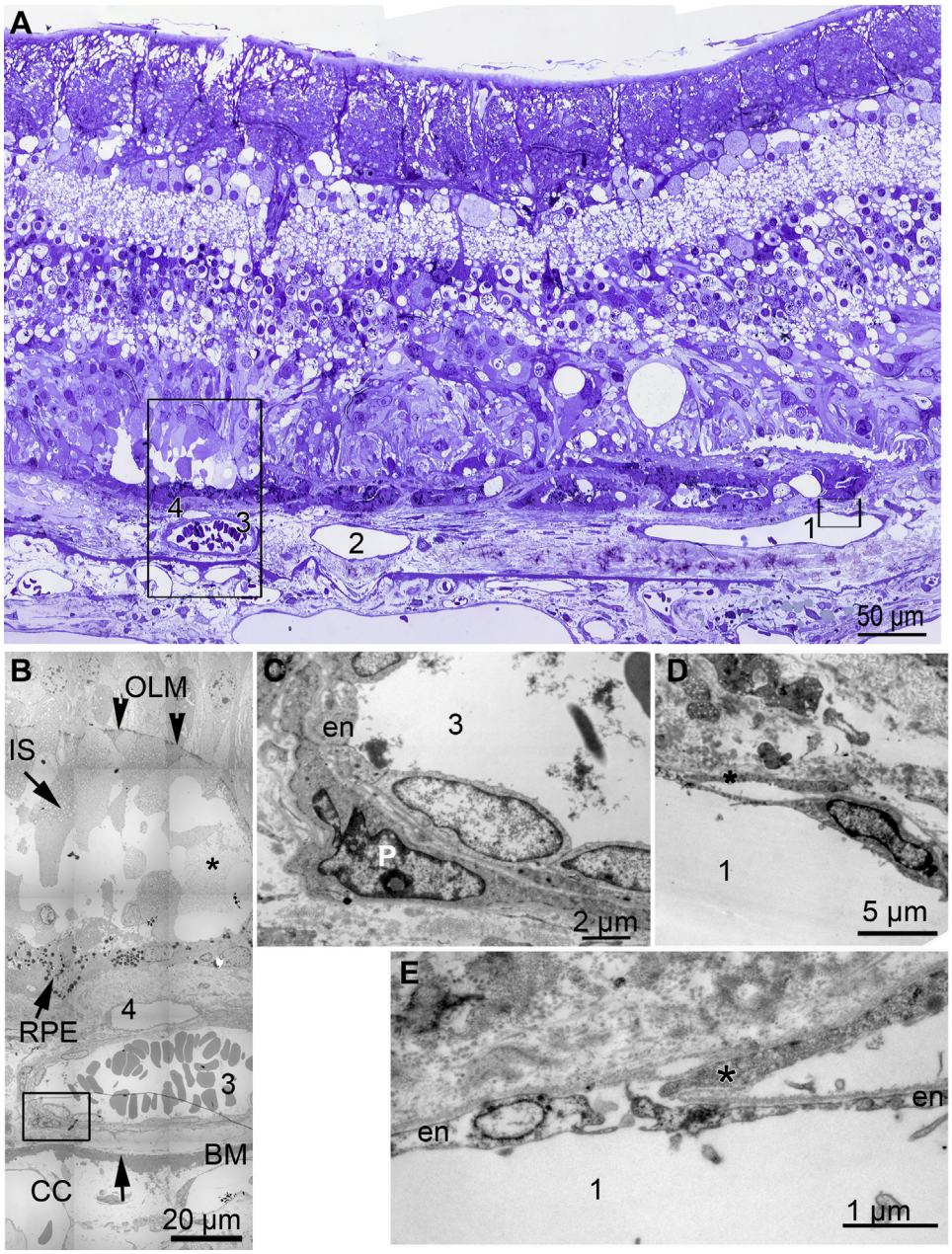

Fig. 6. Choroidal neovascularization can support retinal survival in certain areas. (A) Light microscopical panorama image showing an area where photoreceptors with inner segments and RPE can survive, functional CNV vessels (2, 3, 4), one of them with erythrocytes, can be observed (box magnification in B and C). This area is surrounded on both sides by highly atrophied tissue. CNV vessels 1 (and 5, 6, 7, 8 in the Supplementary Fig. 2) show endothelial lesions (magnification in D, E). Note also the broken elastic layer of BM close to vessel 1. (B) Electron microscopical panorama image showing the surviving area in higher magnification. Photoreceptors show an outer limiting membrane (OLM), nuclei, and inner segments (IS) of the photoreceptor cells. Remnants of the outer segments formed reticular drusen (subretinal drusenoid deposit, Curcio et al., 2012) in the subretinal space (*). Between the RPE and the elastic layer of Bruch's membrane (BM) functional CNV vessels can be observed. CC choriocapillaris (C) Higher magnification of the box in B showing CNV vessel 3 with the typical architecture of an intact and functional vessel: it has a thicker endothelial wall (en) compared with the other CNV vessels. The lumen is open and wide and contains red blood cells. On the left border, a pericyte (P) can be observed. It is separated from the vessel and covered by the same basal membrane. (D) CNV vessel 1 shows an intact endothelium in about 75% of the vessel area. However, some cells appear abnormal, for example, a fibroblastic cell of unknown origin (*) is connected to the endothelial cells of the vessel wall and they are covered by the same basal membrane. (E) With higher magnification it can be observed that the endothelial cells lack cell connections and are thus leaky. In addition, the left endothelial cell is disintegrating. Abbreviations: CNV, choroidal neovascularization; RPE, retinal pigment epithelium.

changes with AMD progression were investigated at transitions between 2 stages. Seven AMD donors showed such transitions (Table 1). As an example, the mean values for transitions between stage II and IV and transitions between stage II and V are illustrated in Fig. 7. RPE and CC loss from stage II to stage IV are significant. The data indicate also that the CC is always more damaged in stage II compared with the RPE (NS) suggesting first loss of CC followed by RPE. It also shows that the RPE in stage II of donors with GA is already more damaged compared with the RPE in stage II of CNV.

In Fig. 8A, the transition data were resorted according to the single stages (independent of their transition partner stage) yielding changes to the RPE and CC with AMD progression.

The data confirm the results of Fig. 7 and additionally prove that even control sections could suffer from initial loss of intact vessels with an otherwise intact RPE layer. This is also illustrated in the

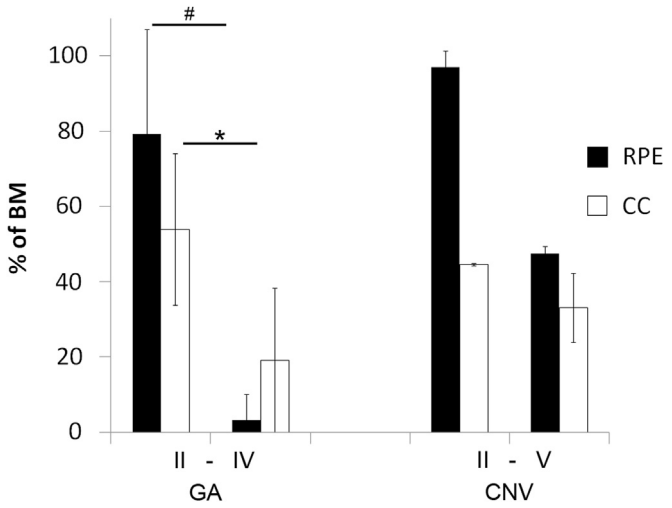

Fig. 7. The presence of CC and RPE in transitions between stage II and stage IV in the case of GA (n = 5 donors) and stage II and stage V in the case of CNV (n = 2 donors), respectively. Only those donors were included that show exactly one of the 2 types of transitions. Presented are mean values and standard deviations. * $p = 0.04$ for CC stage II–IV; # $p = 0.01$ for RPE stage II–IV; the CC and RPE loss in GA (II–IV) were positively correlated according to linear regression analysis of the single values ($R^2 = 0.57$). *p*-values for transitions between stage II and V were not statistically significant because of the small sample number. Abbreviations: CC choriocapillaris; CNV, choroidal neovascularization; GA, geographic atrophy; RPE, retinal pigment epithelium.

corresponding correlation diagram (Fig. 8B), which also shows the high interdependency of the RPE and CC values ($R^2 = 0.89$ for mean values of the stages; $R^2 = 0.57$ for their original data). For further correlation of CC with RPE loss within or between the individual stages, Tables 5–7.

To investigate whether the RPE or CC was surviving whereas the other one had already disappeared, those areas were measured where either the RPE or the CC, both or none of these layers were lost. For better understanding refer to Fig. 9A. Fig. 9B–C illustrates the relation of the present and lost RPE and CC for the different stages of destruction in dry and wet AMD and for control sections. Again, sections which appeared normal at first sight already contained areas where the CC area was decreased (control and stage I [0%–30%]). This can only be investigated using detailed analyses as performed in Fig. 9. In early AMD (stage II) of both wet and dry AMD donors, RPE cells also showed first lesions but CC area loss was still more prominent. In wet AMD (Stage III, V), the CC was affected more severely compared with the RPE, which was counterbalanced by blood vessel outgrowth.

4. Discussion

The main focus of the present work was to find out whether RPE or CC loss precedes retinal degeneration with AMD, independent of the AMD type. Already in the late 60s, scientists were discussing whether the CC (Duke-Elder, 1966) or BM and RPE (Hogan, 1967, 1972) were the initiators of AMD (Sarks, 1976). However, this question still remains to be solved as the RPE and CC share a mutualistic relationship (Bhutto and Lutty, 2012).

Early AMD is described as affecting primarily the RPE and Bruch's membrane. Changes in the RPE are thought to lead to oxidative stress and deposition of undegradable material between the RPE and Bruch's membrane, where it can build basal deposits and large drusen. However, drusen formation can also occur as a result of normal physiological outflow stopped by a barrier yielding particle fusion and formation of lipoprotein-derived debris, which does not have to be oxidized. This "response-to-retention" model reflects the likely source of soft drusen and basal linear deposits more accurately (Curcio et al., 2011).

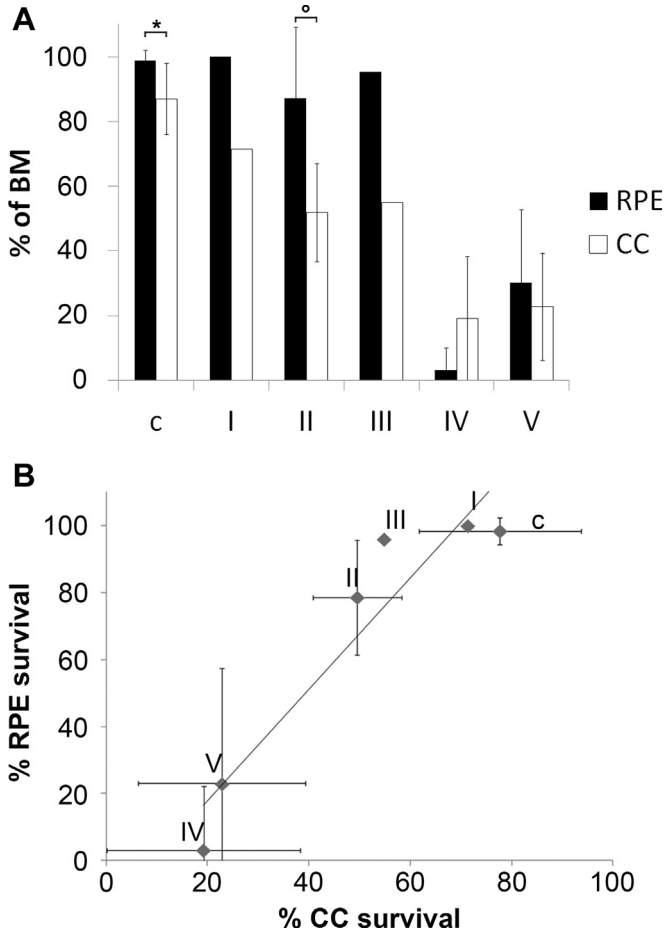

Fig. 8. The presence of CC and RPE in relation to the length of BM sorted by stage. (A) Controls (c) already show a slightly decreased CC compared with RPE (* $p = 0.01$). In the AMD stages I–III, this effect is even more obvious (e.g., stage II ° $p = 0.007$). Stage IV GA shows lower values for RPE, respectively (NS). Note, that data are only taken from transition stages, that is, for control n = 10 areas of 5 donors (10/5); stage I n = 1/1, stage II n = 9/7, stage III n = 1/1, stage IV n = 5/5, and stage V n = 4/3. Statistics for transitions from II to IV, II to V, and IV to V are shown in Table 6. (B) Positive correlation of the survival of RPE and CC in the different AMD stages and controls ($R^2 = 0.89$). Abbreviations: AMD, age-related macular degeneration; BM, Bruch's membrane; CC choriocapillaris; GA, geographic atrophy; RPE, retinal pigment epithelium.

Together with increasing thickness of BM with age, these deposits are responsible for diminished transport of nutrients and metabolites through the blood-retinal barrier leading to more oxidative stress in the retina-choroid complex. Finally, these cumulative reactions may result in (dry) AMD. In this scenario, the main initiator is supposed to be the RPE, but meanwhile the occurrence of deposits and drusen was also correlated to the capillary layer of the choroid, the choriocapillaris. It was found that deposits often form at the pillars between single CC vessels (Kochounian et al., 2009; Lengyel et al., 2004; Sarks, 1999), where a rapid removal of the material by the bloodstream is inhibited. A concurrent thinning (Margolis and Spaide, 2009) and loss of capillaries with age is discussed controversially (Jonas et al., 2014), but would further lead to impaired blood perfusion (Grunwald et al., 1998) and probably also to additional waste accumulation in BM. This impaired blood perfusion is further increased with AMD (Machalinska et al., 2011; Metelitsina et al., 2008; Mullins et al., 2011). Others found elevated levels of circulating endothelial cells as a marker of chronical vascular dysfunction in both wet and dry AMD patients (Machalinska et al., 2011).

In our opinion, in wet AMD, the loss of the CC is counteracted by the formation and growth of new blood vessels into the

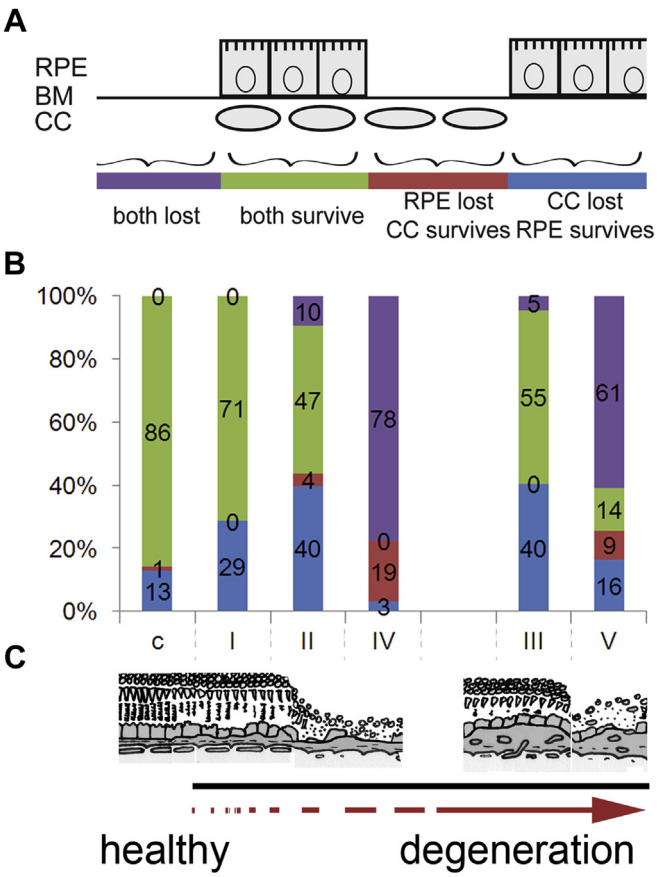

Fig. 9. The order of CC and RPE loss. (A) The presence ("survival") of RPE and CC per μm of BM was measured. Areas where both layers were lost were labeled violet in the diagram in part (B). Areas where both layers were present were labeled green. Areas where only the RPE was lost whereas the underlying CC was still there were labeled red. Vice versa, areas where the RPE was still there but the underlying CC lost were stained blue. (B) The diagram shows the mean values of the previously mentioned 4 situations per stage. Controls and stage I sections thus show both the surviving RPE and CC in over 70% of the area investigated. There are no areas where both layers were missing; however, in about 13% (control) and 29% (Stage I) the CC was missing although the RPE was still there. Also stage III, the initial stage of wet AMD still showed a high amount of viable RPE and CC (over 50%), but the CC was already highly impaired (40% + 5% where both layers are already completely lost). In the late stages of AMD (IV, V), most of the areas investigated had completely degenerated (violet). Depending on the AMD type either the RPE (dry AMD; IV) or the CC (wet AMD; V) was additionally affected more severely. Control (c) n = 10 areas of 5 donors (10/5); I, n = 1/1; II, n = 9/7; III, n = 1/1; IV, n = 5/5; and V, n = 4/3. (C) The scheme of degenerative stages is presented below the diagram to illustrate the given order of stages for better understanding (see digital version for color images). Statistics are given in Table 7. Abbreviations: AMD, age-related macular degeneration; BM, Bruch's membrane; CC choriocapillaris; RPE, retinal pigment epithelium.

subretinal space where they should substitute the CC function, probably leading to longer survival of the RPE and retina, as indicated in Fig. 6 and Supplementary Fig. 2. Unfortunately, these newly formed blood vessels are often stunted and unfunctional and instead of restoring the transport of metabolites to and from the retina, they promote blood leakage, accumulation of extracellular matrix and the invasion of macrophages and finally lead to scar formation and vision loss (Fig. 6, Supplementary Fig. 2). Our suggestions concerning the extended survival of retinal layers with early CNV are only based on 2 sections investigated in this work and will thus not be discussed further. However, they are in line with the excellent previous work that showed that CNV is a stereotypic and nonspecific wound healing response to a specific stimulus, here AMD (reviewed in Grossniklaus and Green, 2004).

Table 3
Type and frequency of basal deposits

Donor number	Semi	EM	Grade[a]
C1	None	—	0
C2	Patchy-continuous	LAM	1–2
C4	None	—	0
C5	None-patchy	—	0–1
C7	Patchy-continuous	LAM	1–2
C8	Patchy	LIN + LAM	1
C9	None-patchy	—	0–1
A1	Thin-thick continuous	LIN < LAM	2–3
A2	Patchy-thick continuous	NI	1–3
A3	Thick continuous	NI	3
A4	Thick continuous	LIN > LAM	3
A5	Thick continuous	CNV, LIN?	3
A6	Patchy-continuous	LAM	1–2
A7	Thick continuous	LAM	3
A8	Patchy-continuous	LIN < LAM	1–2
A9	Thick continuous	LIN > LAM	3
A10	Thick continuous	CNV, LIN + LAM	3
A11	Thick continuous	LAM	3
A12	Thin-thick continuous	LIN < LAM	2–3

No deposit is indicated by (0), Patchy deposit <125 μm length is indicated by (1), Thin continuous with >125 μm length and <2 μm height is indicated by (2), thick continuous with >2 μm height is indicated by (3).
Key: CNV, choroidal neovascularization; EM, electron microscopy; LAM, laminar; LIN, linear; NI, not investigated.
[a] Grading according to data presented by experts in the field (Curcio et al., 1998; van der Schaft et al., 1992).

4.1. The scheme of degenerative stages

We graded the different eye samples from control and AMD donors according to a scheme, which was adapted from the groundbreaking work of Sarks (1976). She used sections stained for different BM markers to investigate the influence of basal deposits on retinal degeneration. Accordingly, her scheme of 6 degeneration stages included (I) no deposit, (II) patchy deposits, (III) thin continuous deposits, first clumping of pigment, (IV) thick continuous deposits with occult CNV, (V) basal deposits with loss of the overlying RPE (GA), and finally (VI) disciform degeneration in classic CNV. This scheme has been adapted by different groups before, yielding comparable data sets acquired by different methods (Rudolf et al., 2013; Vogt et al., 2011).

The progression of degeneration in this work was graded in 5 stages and as a function of the RPE and retinal damage rather than deposit formation. Nevertheless, the progression of stages was intriguingly similar.

Note that the terms "occult" and "classic" CNV are derived from a fluorescein angiography-based classification system. They were originally defined as areas with "poorly-defined" or "well-demarcated choroidal hyperfluorescent" margins, respectively (as defined by the Macular Photocoagulation Study Group [1991, 1996]). Meanwhile, histologic data and multimodal imaging devices, such

Table 4
Loss of photoreceptors with AMD, whereas controls show complete photoreceptors all over the section lengths, AMD sections showed increasing loss of nuclei < inner < outer segments compared with controls

	Mean ± SD control	Mean ± SD AMD	*p*-value
Photoreceptor nuclei present (>7 rows)	87 ± 19	38 ± 30	**<0.0001**
Inner segments present (% per BM length)	100 ± 0	41 ± 43	**<0.0001**
Outer segments present (% per BM length)	100 ± 0	30 ± 44	**0.0001**

Key: AMD, age-related macular degeneration; BM, Bruch's membrane; SD, standard deviation.

Table 5
Correlation of CC and RPE within single stages

Stage	Correlation	R^2
Stage 2	$y = 0.18x + 38$	0.18
Stage 4	$y = -0.45x + 21$	0.03
Stage 5	$y = 0.36x + 15$	0.55

Key: CC, choriocapillaris; RPE, retinal pigment epithelium.

as spectral domain optical coherence tomography (SD-OCT), show more clearly the lesion composition with wet AMD. Thus, a new classification system has been proposed by Freund et al. (2010) and should be adapted regularly according to the newly emerging criteria. This classification system is based on 3 different types of CNV: (1) Type 1, vessels confined to the sub-RPE space; (2) vessels proliferating through the RPE into the subretinal space; and (3) intraretinal neovascularization. Although we used the definitions used by Sarks (1976), we also included the new nomenclature in the hope that it will spread when used regularly.

4.2. The impact of capillary loss

Loss of CC vessels was observed in all investigated stages, but was more pronounced with late AMD. It was unexpected that control donors also showed loss of capillaries in about 13% of the investigation area. However, increasing variability of CC density, including up to 50% loss in CC in the 10th decade of life (Ramrattan et al., 1994) has also been observed before and would suggest that loss of capillaries with age may be an initiating factor of AMD, thus also making dry AMD a vascular disease (Friedman, 1997; Machalinska et al., 2011; Verhoeff and Grossman, 1937). Also McLeod et al. (2009) investigated the border regions of macular degeneration in comparison with healthy controls and likewise found loss of a viable CC in alkaline phosphatase stained eyes with GA but even more with CNV. In Fig. 3 of McLeod et al. (2009) they also show initial loss of CC in controls. The same is true for Curcio et al., (2000) who investigated RPE and CC atrophy in peripapillary regions of non-AMD donor eyes. They also found preliminary but unsuspicious choriocapillaris loss in areas with an otherwise normal RPE.

Mullins et al. (2011) performed immunohistological investigations on cryosections of early AMD donors and found a decreasing CC density and increased accumulation of deposits with AMD compared with controls. By differentiation of viable (UEA-1 positive) and non-viable "ghost" vessels they also showed that drusen density was negatively correlated to healthy CC density but positively correlated to CC death. But whether drusen formation was the cause or consequence of CC death could not be answered by their studies. Our data are also in accordance with this excellent publication. Although we did not investigate the EEA-1 or alkaline-phosphatase status of our capillaries, we were able to judge CC health by endothelial cell ultrastructure and determined an increasing loss of viable capillaries with age and AMD by measuring significant changes in CC area, length, and fenestration, which is also in accordance with McLeod et al. (2002).

Table 6
Statistics given for data in Fig. 8 (*p*-values)

	CC (%)	RPE (%)
C-II	NS	<0.001
C-IV	<0.0001	<0.0001
C-V	<0.0001	<0.0001
AMD II–IV	0.004	<0.0001
AMD II–V	0.01	0.001
AMD IV–V	NS	0.04

Key: AMD, age-related macular degeneration; CC, choriocapillaris; NS, not significant; RPE, retinal pigment epithelium.

Table 7
Statistics given for data in Fig. 9 (*p*-values)

AMD stages	II–IV	II–V	IV–V
Only CC lost (%)	0.001	0.05	NS
Only RPE lost (%)	0.04	NS	NS
Both survive (%)	0.0001	0.008	NS
Both lost (%)	<0.0001	0.001	NS
Control-AMD	**C-II**	**C-IV**	**C-V**
Only CC lost (%)	0.02	NS	NS
Only RPE lost (%)	NS	0.01	0.02
Both survive (%)	0.001	<0.0001	<0.0001
Both lost (%)	0.1	<0.0001	<0.0001

Key: AMD, age-related macular degeneration; CC, choriocapillaris; NS, not significant; RPE, retinal pigment epithelium.

Although an intense correlation of basal depositions with AMD stages was not intended in this work, the presented data show that a continuous low layer of basal deposits could already be involved in CC loss and AMD onset, and huge drusen might only be a severe form of this condition. Thus, we suggest that CC loss is actually the cause, rather than the effect of drusen. This is also in accordance with the hypothesis that severe deposits grow close to pillars and already impaired CC vasculature. Further outstanding work on deposit formation, composition, and impact on RPE and CC loss in AMD can be obtained in previous publications, (Curcio and Millican, 1999; Lengyel et al., 2007; Russell et al., 2000; Sarks et al., 2007; Spaide and Curcio, 2010; Spraul et al., 1998).

Meanwhile, gene expression analyses demonstrated a clear decrease in the expression of endothelium-expressed genes in eyes of early AMD donors with concomitant increase in RPE-related genes (Whitmore et al., 2013). This work further suggests loss or dedifferentiation of choroidal endothelial cells before the loss of the RPE (Whitmore et al., 2013).

4.3. Impact of the RPE and the value of investigating transitions

As expected and in accordance with the literature, we found a longer survival of the RPE and predominant loss of the CC in CNV and RPE loss with surviving CC in GA. Interestingly, the RPE of stage II in GA donor eyes was more highly impaired compared with the RPE in stage II of CNV donors (Fig. 7) implicating that the progression in either direction, wet or dry, can already be foreshadowed in areas with early degeneration (stage II). Thus, investigation of transitions between early stages I or II to later stages III, IV, and/or V have to be analyzed more thoroughly to understand the regulatory events leading to either dry or wet AMD. However, the transitions were mostly very abrupt (<50 μm distance) and a clear transition zone between surviving photoreceptor and retinal scarring could hardly be observed. Such abrupt transitions with AMD-like changes in the retina–RPE–CC complex were also shown for age-related peripapillary chorioretinal atrophy of eyes without AMD (Curcio et al., 2000). Thus, the first 200 μm of each stage had to be investigated instead and correlated to each other but also to more central areas of each zone. And indeed, values taken at either side of the transitions did differ from values taken in the central parts of the different stages (e.g., the RPE loss was more severe in central parts of a stage compared with its border region to a healthier area, data not shown). The data show the importance of investigating early stages of AMD and their transitions to end stage degeneration, as it is only here that the possible reasons of the progression of the disease become visible. But note that it is only an assumption that the margins of the lesion represent a directional or temporal intermediate between health and disease, as this is not really known.

4.4. Strength and weaknesses of the study

Sample number: Although this study investigated only a small number of donor eyes, the data of the single donors were investigated with high accuracy using light and electron microscopy and they nicely represent a common behavior of degeneration in the RPE and CC of AMD donor eyes. However, statistics applied in this work should be handled with care because of sample size, extensive mixed statistical approaches accounting for dependencies, as those performed by Vogt et al. (2011) were not applicable. Instead, linear regression analyses account for CC and RPE dependency in the different stages.

Reproducibility: Nevertheless, the values for BM thickness and basal deposits (Ramrattan et al., 1994; Spraul et al., 1996), density of CC vessels (Mullins et al., 2011) and the correlation of RPE and CC loss (Bhutto and Lutty, 2012; McLeod et al., 2009) investigated here were very close to results published before by the experts in this field. This shows the high reproducibility of our work in comparison with other morphologic methodologies but also with clinical imaging techniques like optical coherence tomography (OCT) (Brown et al., 2009) or angiography (Curcio et al., 1998), which can also be applied to donor eyes. Thus, a correlation of different light, fluorescence, and electron microscopical work is of high value.

Postmortem effects: Note that postmortem times could affect ultrastructure especially that of blood vessels yielding collapsed lumina or invisibility of fenestrations. However, this would affect both controls and AMD donors, and it is not the case here, as shrunken vessels mostly show still intact margins like cell membranes, fenestration and a basal lamina, and appear thus morphologically viable (Fig. 3). In addition, they are facing neighboring intact vessels without damage. Besides, the approach used in this work is not solely based on vessel lumen area but addresses the whole CC layer integrity ("length/BM"), which would not be changed by postmortem artefacts. Both approaches show an about 60% loss CC in AMD compared with controls.

Correlative light and electron microscopy: The combination of light and electron microscopy in neighboring sections of the same tissue block is only possible in plastic sections (here epon) and was a great plus, as both the overview information and the ultrastructural resolution complement each other. They show per se an excellent contrast and ultrastructure compared with stained paraffin or frozen sections. Thus, ghost vessels can be recognized without further staining. However, other cell types, such as those present in BM, can only be fully addressed with antibody labeling which was not performed here. In addition, all histologic analyses represent only one stage in time, thus a progression over time cannot be addressed by either of the discussed methods.

Grading: Our grading primarily addressed the presence of cell layers rather than the viability and/or morphology of these cells. However, it is an estimate of where RPE cells in particular were still viable enough to remain at their destined position, and where organelles like the melanosomes could still participate in antioxidative defense and retinal survival.

Nevertheless, the work shows a practicable method for the investigation of AMD progression. It addresses the importance of investigating border areas between healthy and atrophied regions in AMD samples. With this approach, we showed that loss of choriocapillaris vessels with age occurs and could serve as an indicator and prevalence factor for AMD.

4.5. Summary

Initial CC breakdown is shown to precede RPE and retinal degeneration, as judged from the comparison of control and AMD sections in different stages of destruction. Thus, AMD is presumed to be a vascular disease as has already been postulated before (Friedman, 1997; Verhoeff and Grossman, 1937). Special emphasis should be laid on AMD sections where different stages of degeneration pass over into each other. By comparing these interfaces using the given approach, a possible sequence of degenerative steps with aging and AMD can be revealed.

Disclosure statement

The authors have no actual or potential conflicts of interest including financial, personal, or other relationships with other people or organizations within 3 years of beginning this work submitted that could inappropriately influence their work. Written informed consent of the eye donors for use in medical research and approval of the Institutional Review Board of the University of Tuebingen were obtained.

Acknowledgements

The authors thank Prof Dr Joe Hollyfield and Dr Vera Bonilha (Retinal Degeneration Histopathology Laboratory, Cole Eye Institute —The Cleveland Clinic Foundation) for their kind help in providing them with AMD donor eyes. They also thank the collegues of Dr Yoeruek, namely, Dr Max Warga, Johanna Hofmann, and Dr Barbara Wallenfels-Thilo of the Cornea Bank Tuebingen, and Dr Bernhard Hirt of the Department of Anatomy Tuebingen for providing them with the control eyes. They are indebted to the donors and their families for allowing the use of their eyes in reseach. They thank Sigrid Schultheiss for excellent technical assistance and Judith Birch for proof reading. This work was supported by the following grants: Deutsche Forschungsgemeinschaft BI 1551/2-1, fortuene 1957-0-0, and fortuene 2062-0-0.

Supplementary data

Supplementary data associated with this article can be found, in the online version, at http://dx.doi.org/10.1016/j.neurobiolaging.2014.05.003.

References

Bhutto, I., Lutty, G., 2012. Understanding age-related macular degeneration (AMD): relationships between the photoreceptor/retinal pigment epithelium/Bruch's membrane/choriocapillaris complex. Mol. Aspects Med. 33, 295–317.

Brown, N.H., Koreishi, A.F., McCall, M., Izatt, J.A., Rickman, C.B., Toth, C.A., 2009. Developing SDOCT to assess donor human eyes prior to tissue sectioning for research. Graefes Arch. Clin. Exp. Ophthalmol. 247, 1069–1080.

Brown, W.R., Thore, C.R., 2010. Review: cerebral microvascular pathology in ageing and neurodegeneration. Neuropathol. Appl. Neurobiol. 37, 56–74.

Curcio, C.A., Johnson, M., Rudolf, M., Huang, J.D., 2011. The oil spill in ageing Bruch membrane. Br. J. Ophthalmol. 95, 1638–1645.

Curcio, C.A., Medeiros, N.E., Millican, C.L., 1998. The Alabama age-related macular degeneration grading system for donor eyes. Invest Ophthalmol. Vis. Sci. 39, 1085–1096.

Curcio, C.A., Messinger, J.D., Sloan, K.R., McGwin, G., Medeiros, N.E., Spaide, R.F., 2012. Subretinal drusenoid deposits in non-neovascular age-related macular degeneration: morphology, prevalence, topography, and biogenesis model. Retina 33, 265–276.

Curcio, C.A., Millican, C.L., 1999. Basal linear deposit and large drusen are specific for early age-related maculopathy. Arch. Ophthalmol. 117, 329–339.

Curcio, C.A., Saunders, P.L., Younger, P.W., Malek, G., 2000. Peripapillary chorioretinal atrophy: Bruch's membrane changes and photoreceptor loss. Ophthalmology 107, 334–343.

Duke-Elder, S., 1966. System of Ophthalmology. Kimpton, London, p. 610.

Freund, K.B., Zweifel, S.A., Engelbert, M., 2010. Do we need a new classification for choroidal neovascularization in age-related macular degeneration? Retina 30, 1333–1349.

Friedman, E., 1997. A hemodynamic model of the pathogenesis of age-related macular degeneration. Am. J. Ophthalmol. 124, 677–682.

Green, W.R., Enger, C., 1993. Age-related macular degeneration histopathologic studies. The 1992 Lorenz E. Zimmerman Lecture. Ophthalmology 100, 1519–1535.

Grossniklaus, H.E., Green, W.R., 2004. Choroidal neovascularization. Am. J. Ophthalmol. 137, 496–503.
Grunwald, J.E., Hariprasad, S.M., DuPont, J., Maguire, M.G., Fine, S.L., Brucker, A.J., Maguire, A.M., Ho, A.C., 1998. Foveolar choroidal blood flow in age-related macular degeneration. Invest Ophthalmol. Vis. Sci. 39, 385–390.
Herrmann, P., Holz, F.G., Charbel Issa, P., 2013. Etiology and pathogenesis of age-related macular degeneration. Ophthalmologe 110, 377–387; quiz 388–9.
Hogan, M.J., 1967. Bruch's membrane and disease of the macula. Role of elastic tissue and collagen. Trans. Ophthalmol. Soc. U.K 87, 113–161.
Hogan, M.J., 1972. Role of the retinal pigment epithelium in macular disease. Trans. Am. Acad. Ophthalmol. Otolaryngol. 76, 64–80.
Jonas, J.B., Forster, T.M., Steinmetz, P., Schlichtenbrede, F.C., Harder, B.C., 2014. Choroidal thickness in age-related macular degeneration. Retina 34, 1149–1155.
Kochounian, H., Johnson, L.V., Fong, H.K., 2009. Accumulation of extracellular RGR-d in Bruch's membrane and close association with drusen at intercapillary regions. Exp. Eye Res. 88, 1129–1136.
Kocur, I., Resnikoff, S., 2002. Visual impairment and blindness in Europe and their prevention. Br. J. Ophthalmol. 86, 716–722.
Lengyel, I., Flinn, J.M., Peto, T., Linkous, D.H., Cano, K., Bird, A.C., Lanzirotti, A., Frederickson, C.J., van Kuijk, F.J., 2007. High concentration of zinc in sub-retinal pigment epithelial deposits. Exp. Eye Res. 84, 772–780.
Lengyel, I., Tufail, A., Hosaini, H.A., Luthert, P., Bird, A.C., Jeffery, G., 2004. Association of drusen deposition with choroidal intercapillary pillars in the aging human eye. Invest Ophthalmol. Vis. Sci. 45, 2886–2892.
Liu, M.M., Chan, C.C., Tuo, J., 2012. Genetic mechanisms and age-related macular degeneration: common variants, rare variants, copy number variations, epigenetics, and mitochondrial genetics. Hum. Genomics 6, 13.
Loffler, K.U., Lee, W.R., 1986. Basal linear deposit in the human macula. Graefes Arch. Clin. Exp. Ophthalmol. 224, 493–501.
Lutty, G., Grunwald, J., Majji, A.B., Uyama, M., Yoneya, S., 1999. Changes in choriocapillaris and retinal pigment epithelium in age-related macular degeneration. Mol. Vis. 5, 35.
Machalinska, A., Safranow, K., Sylwestrzak, Z., Szmatloch, K., Kuprjanowicz, L., Karczewicz, D., 2011. Elevated level of circulating endothelial cells as an exponent of chronic vascular dysfunction in the course of AMD. Klin Oczna 113, 228–232.
Macular Photocoagulation Study Group, 1991. Laser photocoagulation of subfoveal neovascular lesions in age-related macular degeneration. Results of a randomized clinical trial. Arch. Ophthalmol. 109, 1220–1231.
Macular Photocoagulation Study Group, 1996. Occult choroidal neovascularization. Influence on visual outcome in patients with age-related macular degeneration. Arch. Ophthalmol. 114, 400–412.
Margolis, R., Spaide, R.F., 2009. A pilot study of enhanced depth imaging optical coherence tomography of the choroid in normal eyes. Am. J. Ophthalmol. 147, 811–815.
McLeod, D.S., Grebe, R., Bhutto, I., Merges, C., Baba, T., Lutty, G.A., 2009. Relationship between RPE and choriocapillaris in age-related macular degeneration. Invest Ophthalmol. Vis. Sci. 50, 4982–4991.
McLeod, D.S., Taomoto, M., Otsuji, T., Green, W.R., Sunness, J.S., Lutty, G.A., 2002. Quantifying changes in RPE and choroidal vasculature in eyes with age-related macular degeneration. Invest Ophthalmol. Vis. Sci. 43, 1986–1993.
Metelitsina, T.I., Grunwald, J.E., DuPont, J.C., Ying, G.S., Brucker, A.J., Dunaief, J.L., 2008. Foveolar choroidal circulation and choroidal neovascularization in age-related macular degeneration. Invest Ophthalmol. Vis. Sci. 49, 358–363.
Mullins, R.F., Johnson, M.N., Faidley, E.A., Skeie, J.M., Huang, J., 2011. Choriocapillaris vascular dropout related to density of drusen in human eyes with early age-related macular degeneration. Invest Ophthalmol. Vis. Sci. 52, 1606–1612.
Prokofyeva, E., Zrenner, E., 2011. Epidemiology of major eye diseases leading to blindness in Europe: a literature review. Ophthalmic Res. 47, 171–188.
Ramrattan, R.S., van der Schaft, T.L., Mooy, C.M., de Bruijn, W.C., Mulder, P.G., de Jong, P.T., 1994. Morphometric analysis of Bruch's membrane, the choriocapillaris, and the choroid in aging. Invest Ophthalmol. Vis. Sci. 35, 2857–2864.
Rudolf, M., Vogt, S.D., Curcio, C.A., Huisingh, C., McGwin Jr., G., Wagner, A., Grisanti, S., Read, R.W., 2013. Histologic basis of variations in retinal pigment epithelium autofluorescence in eyes with geographic atrophy. Ophthalmology 120, 821–828.
Russell, S.R., Mullins, R.F., Schneider, B.L., Hageman, G.S., 2000. Location, substructure, and composition of basal laminar drusen compared with drusen associated with aging and age-related macular degeneration. Am. J. Ophthalmol. 129, 205–214.
Sarks, S., Cherepanoff, S., Killingsworth, M., Sarks, J., 2007. Relationship of Basal laminar deposit and membranous debris to the clinical presentation of early age-related macular degeneration. Invest Ophthalmol. Vis. Sci. 48, 968–977.
Sarks, S.H., 1976. Ageing and degeneration in the macular region: a clinico-pathological study. Br. J. Ophthalmol. 60, 324–341.
Sarks, S.H., A, J.J., Killingsworth, M.C., Sarks, J.P., 1999. Early drusen formation in the normal and aging eye and their relation to age related maculopathy: a clinicopathological study. Br. J. Ophthalmol. 83, 358–368.
Sierra, C., 2012. Cerebral small vessel disease, cognitive impairment and vascular dementia. Panminerva Med. 54, 179–188.
Spaide, R.F., Curcio, C.A., 2010. Drusen characterization with multimodal imaging. Retina 30, 1441–1454.
Spraul, C.W., Lang, G.E., Grossniklaus, H.E., 1996. Morphometric analysis of the choroid, Bruch's membrane, and retinal pigment epithelium in eyes with age-related macular degeneration. Invest Ophthalmol. Vis. Sci. 37, 2724–2735.
Spraul, C.W., Lang, G.E., Grossniklaus, H.E., Lang, G.K., 1998. Characteristics of drusen and changes in Bruch's membrane in eyes with age-related macular degeneration. Histological study. Ophthalmologe 95, 73–79.
van der Schaft, T.L., Mooy, C.M., de Bruijn, W.C., Oron, F.G., Mulder, P.G., de Jong, P.T., 1992. Histologic features of the early stages of age-related macular degeneration. A statistical analysis. Ophthalmology 99, 278–286.
Verhoeff, F.H., Grossman, H.P., 1937. The pathogenesis of disciform degeneration of the macula. Trans. Am. Ophthalmol. Soc. 35, 262–294.
Vogt, S.D., Curcio, C.A., Wang, L., Li, C.M., McGwin Jr., G., Medeiros, N.E., Philp, N.J., Kimble, J.A., Read, R.W., 2011. Retinal pigment epithelial expression of complement regulator CD46 is altered early in the course of geographic atrophy. Exp. Eye Res. 93, 413–423.
Whitmore, S.S., Braun, T.A., Skeie, J.M., Haas, C.M., Sohn, E.H., Stone, E.M., Scheetz, T.E., Mullins, R.F., 2013. Altered gene expression in dry age-related macular degeneration suggests early loss of choroidal endothelial cells. Mol. Vis. 19, 2274–2297.